ISIJ International, Vol. 62 (2022), No. 4, pp. 708–713
https://doi.org/10.2355/isijinternational.ISIJINT-2021-503

Heat Transfer via Laminar Jet Flow from Upward-facing Triple-pipe System onto Hot Moving Thin Steel Sheet

Junya NAKAHARA,[1)] Katsutoshi TATEBE[1)]* and Hitoshi FUJIMOTO[2)]

1) Graduate School of Energy Science, Kyoto University. Now at Research & Development, Process Research Laboratories, Nippon Steel Corporation, 20 -1 Shintomi, Futtsu, Chiba, 293-8511 Japan.
2) Graduate School of Energy Science, Kyoto University, Sakyo-ku, Kyoto, 606-8501 Japan.

(*Received on October 15, 2021; accepted on December 23, 2021*)

With the primary objective of investigating the effect of varying the nozzle interval and steel sheet temperature on the heat flux distribution within the jet impact region, the boiling heat transfer characteristics of three upward-facing water jets impinging on a moving hot thin steel sheet were studied as a fundamental phenomenon of run-out table (ROT) cooling in a hot rolling mill. Using water as a test coolant and a stainless steel sheet as a test piece, the intervals between adjacent nozzles were varied from 8 to 12 to 16 mm and experiments were conducted over a steel sheet temperature range of 300–700°C and at a moving velocity and volume flow rate of 1.5 m/s and 960 ml/min, respectively. Three-dimensional inverse heat conduction analysis was used to evaluate the heat flux distribution based on the temperature profile of the steel sheet captured by a thermal imaging camera. It was found that three high-heat flux regions were present in the jet impact region, with the heat flux highly dependent on the temperature of the steel sheet associated with the boiling mode. In addition, it was found that, because of the effects of the two side jets on the flow formed by the center jet, the high-heat-flux region associated with the center jet was dependent on the nozzle interval. As a result of this dependence, decreases in the nozzle interval reduced the degree of heat removal by the center jet.

KEY WORDS: boiling heat transfer; multiple jet impingement to moving solid; inverse heat conduction analysis.

1. Introduction

In run-out-table (ROT) cooling in hot rolling mills, hot moving steel sheets are rapidly cooled from 800–900°C to a cooling-stop temperature in accordance with a pre-determined cooling schedule.[1–3)] To fabricate steel products with pre-determined mechanical properties, it is necessary to accurately control the temperature of the steel sheet during the cooling process. Water jet arrays are typically used as cooling systems, as simultaneous jet impingement on the top and bottom surfaces of a moving hot steel sheet can remove a significant amount of heat at the jet impact points. As the point of impact of each jet on the steel sheet shifts in the direction of motion over time, the steel surface is most effectively cooled when it passes below a jet and less effectively cooled at other times. Consequently, the process of cooling a moving steel sheet involves repetition of this heat removal pattern.

As the temperature of the moving steel sheet is far above the boiling temperature of water, the occurrence of flow boiling, which in turn produces complex hydrodynamics, is inevitable. Recent review papers on the boiling heat transfer characteristics of water jet impingement on hot solids[1–5)] have revealed that many prior studies on the cooling characteristics of jet impingement focused on hot static solids impacted by water jets at stationary points. As the cooling process for a static solid is apparently different from that in ROT cooling, predicting the actual ROT cooling process requires measurement of the heat transfer to a moving hot solid. Recent studies on liquid jet impingement on moving hot solids[6–11)] have revealed that the heat transfer characteristics vary as a result of factors including water flow rate and the temperature and moving velocity of the solid. However, there is still a lack of fundamental knowledge, particularly in the transition boiling regime.

Conventionally, the removal of heat by jet impingement is evaluated by solving the inverse heat conduction problem using temperatures measured in the solid; by increasing the number of measurement points in solving the multidimensional heat conduction equation, the results of this process become more accurate. However, typical measurement devices such as thermocouples can measure only single

* Corresponding author: E-mail: tatebe.7gd.katsutoshi@jp.nipponsteel.com

local temperatures, making them unsuitable for practically measuring heat flux distributions with high spatial resolution.

To address these issues, the authors have developed a method capable of evaluating the heat flux distributions in the jet impact region with higher spatial resolution than previous approaches.[12–15] The proposed method involves measurement of the temperature of a steel surface via thermography and three-dimensional inverse heat conduction analysis in the steady state. To develop this method, the authors studied the heat transfer characteristics of downward-facing single jets[12,13] and multiple-jet arrays[14] and upward-facing single jets[15] impinging on moving solids.

In this study, the heat transfer characteristics of a triple upward-facing jet array impinging on a moving hot solid were experimentally analyzed using 17°C water as a test coolant shot from three jets aligned along the width direction of a stainless steel sheet (SUS430), which was moving at 1.5 m/s and heated to an initial temperature varying from 300 to 700°C. The primary objective was to explore the effect of varying the nozzle interval on the characteristics of heat transfer from a central jet whose hydrodynamics are influenced by two neighboring jets. In addition, the effects of varying the temperature of the test sheet were investigated in detail. Finally, the fundamental heat transfer characteristics obtained from our experimental data were compared with those for single-jet upward impingement.[15]

2. Experiment

Figure 1 shows a schematic of the experimental apparatus used to study the boiling heat transfer characteristics of three upward-facing jets impinging on a moving hot solid. The apparatus comprised a moving steel sheet mounted on a linear motor actuator, a water supply system for feeding the three jets, and observational equipment. The setup, experimental procedure, and data reduction method were very similar to those used in our previous work[15] on upward single-jet impingement.

Water at a temperature of 17°C was used as test coolant. Three identical pipe nozzles with inner diameters of 4 mm were aligned along the width direction of the moving test sheet with the nozzle spacing set to $d_n = 8$, 12, or 16 mm. The length of the pipe was 500 mm. A flow-disturbing mesh was inserted into the inlet of each nozzle to form a fully developed turbulent pipe flow near its mouth. The flow rate of water was measured directly from the volume of water discharged from each nozzle during the sampling period (= 60 s). The nozzle-to-test sheet distance was set to 12 mm.

The steel test sheet was fabricated from stainless steel (SUS430) and had the dimensions 60 mm × 220 mm × 0.3 mm (width × length × thickness), as shown in Fig. 1. To prevent unwanted deformation from thermal stress during the experiments, both of the longer sides of the sheet were bent at right angles 5 mm from the edge. At the beginning of each run, the test sheet was heated to a preset temperature via direct resistance heating with a DC power supply and then transported into the test section by a linear motor actuator with a preset velocity.

An infrared camera that could capture thermal images with a resolution of 320 × 240 pixels was used to measure the temperature profile of the opposite side of the cooling surface, to which a thin coat of black body paint with an emissivity of 0.94 had been added to ensure accurate measurement of temperature. The infrared camera was fixed 300 mm above the moving test sheet and captured images in which each pixel corresponded to approximately 0.6 mm. The exposure time of the camera was 1/60 s, and one thermal image was captured per run. The camera was calibrated using a thermocouple attached to the test surface, as shown in Fig. 1.

A digital camera with an effective spatial resolution of 4 752 × 2 592 pixels was used to observe the coolant flow; although not shown in Fig. 1, it was set obliquely below the moving test sheet. A flash photography technique was adopted to capture the instantaneous motion of water jet impingement.

To evaluate the heat flux distribution on the cooling surface, the inverse heat conduction problem was numerically solved by applying a finite volume technique using the measured temperature profile of the opposite side as the boundary condition. The heat conduction equation inside the

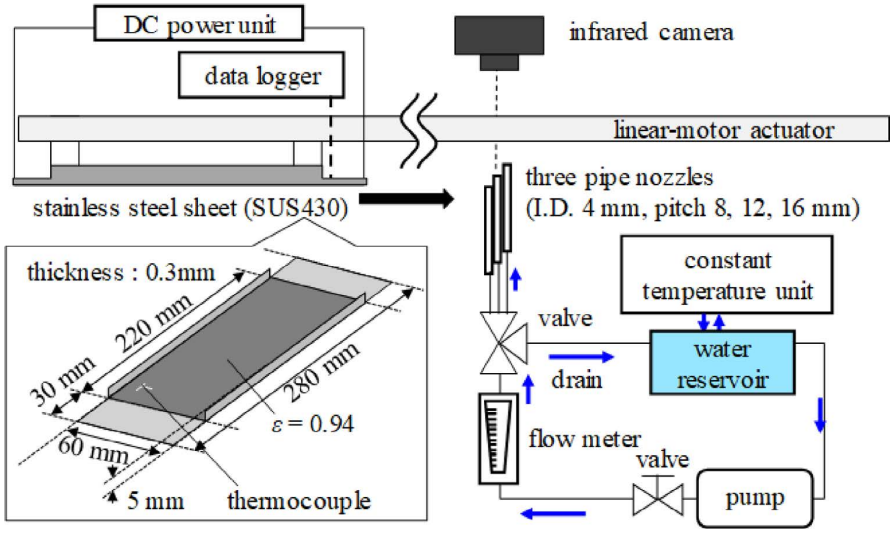

Fig. 1. Schematic of experimental apparatus. (Online version in color.)

test sheet in a spatially fixed three-dimensional Cartesian coordinate system is given by

$$\rho_p c_p \left(\frac{\partial T}{\partial t} + V_s \frac{\partial T}{\partial x} \right) = \lambda_p \left(\frac{\partial^2 T}{\partial x^2} + \frac{\partial^2 T}{\partial y^2} + \frac{\partial^2 T}{\partial z^2} \right), \quad \text{..... (1)}$$

where t, T, V_s, ρ_p, c_p, and λ_p represent the time, local temperature, velocity of motion of the test sheet, material density, specific heat, and thermal conductivity, respectively, and the coordinates (x, y, z) indicate the direction of motion of the steel sheet, the width direction, and the thickness direction, respectively. The temperature profile is assumed to be steady in the spatially fixed three-dimensional Cartesian coordinate system except in the front edge region of moving test sheet, because the sheet temperature upstream of the jet impact point, the moving velocity of test sheet, the jet velocity were maintained to preset values during each run. Thus, the first term on the left hand side in Eq. (1) is neglected for evaluating heat transfer characteristics. The following equation was used for data reduction:

$$\rho_p c_p V_s \frac{\partial T}{\partial x} = \lambda_p \left(\frac{\partial^2 T}{\partial x^2} + \frac{\partial^2 T}{\partial y^2} + \frac{\partial^2 T}{\partial z^2} \right). \quad \text{..... (2)}$$

The temperature dependencies of the properties listed above are considered when solving Eq. (2). More information concerning the experimental procedure and data reduction method is provided in our previous work.[15)]

The initial temperature of the test sheet was varied from T_s = 300 to 700°C. The volume flow rate of water for each jet was fixed at Q = 960 ml/min (2 880 ml/min total for all three jets) and the corresponding mean jet velocity at the nozzle exit was 1.27 m/s. Also, the jet impact velocity taking account of gravitational acceleration was 1.19 m/s. The velocity of the test sheet was set to 1.5 m/s. Although we attempted to conduct experiments at larger water flow rates and smaller test sheet velocities, these attempts were unsuccessful as a result of unwanted local buckling of the test sheet owing to abrupt thermal stress induced by the jet impact; because this local buckling resulted in irregular coolant flows, the experimental results were omitted.

3. Results and Discussion

Figure 2 shows the hydrodynamic behavior of the water jets captured by flash-photography at initial test sheet temperatures of T_s = 300–700°C and nozzle spacings of d_n = 8 and 16 mm. The results for d_n = 8 mm and T_s = 300°C are not shown because unwanted distortion of the steel sheets occurred under these conditions. It is also noted that only one nozzle of the three-jet array is exposed in each figure owing to the positioning of the camera (see also the schematic in the figure). In the figures, radially spreading water films form along the test sheet from the jet impact points and peel off from the moving test sheet under the force of gravity. A pair of thin vertical water films are observed between each of the two side jets as a result of the flow interaction (see also **Fig. 3**). At T_s = 300°C, the water film in the jet impact region appears to be very cloudy as a result of numerous vapor bubbles and/or small droplets scattering the observation light: in other words, strong nucleate boiling occurs. The liquid film becomes transparent with increasing initial sheet temperature, suggesting that the dominant boiling mode in the jet impact region varies from strong nucleate to film boiling. At 700°C, the test sheet is hot red and three linear dark areas appear in the direction of motion.

Figure 4 shows the measured temperature profiles of the noncooled surface. The three black points plotted in each

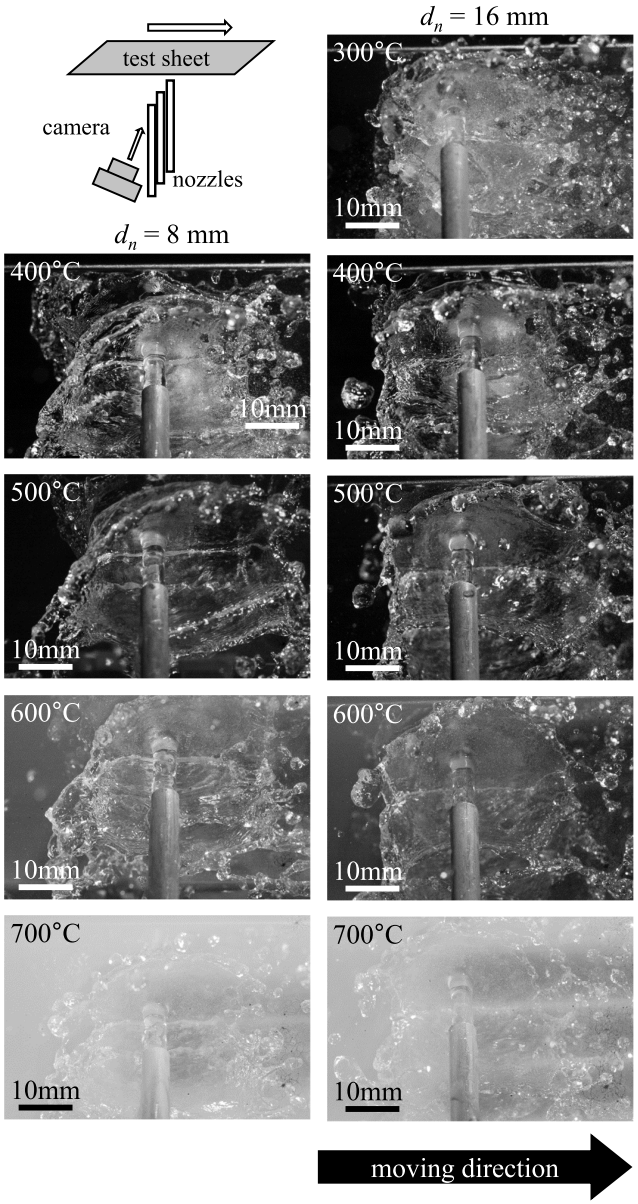

Fig. 2. Water flow motion captured by flash-photography technique.

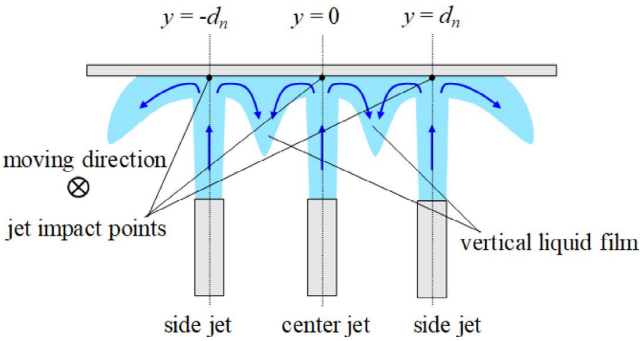

Fig. 3. Schematic of flow motion of three-jet impingement. (Online version in color.)

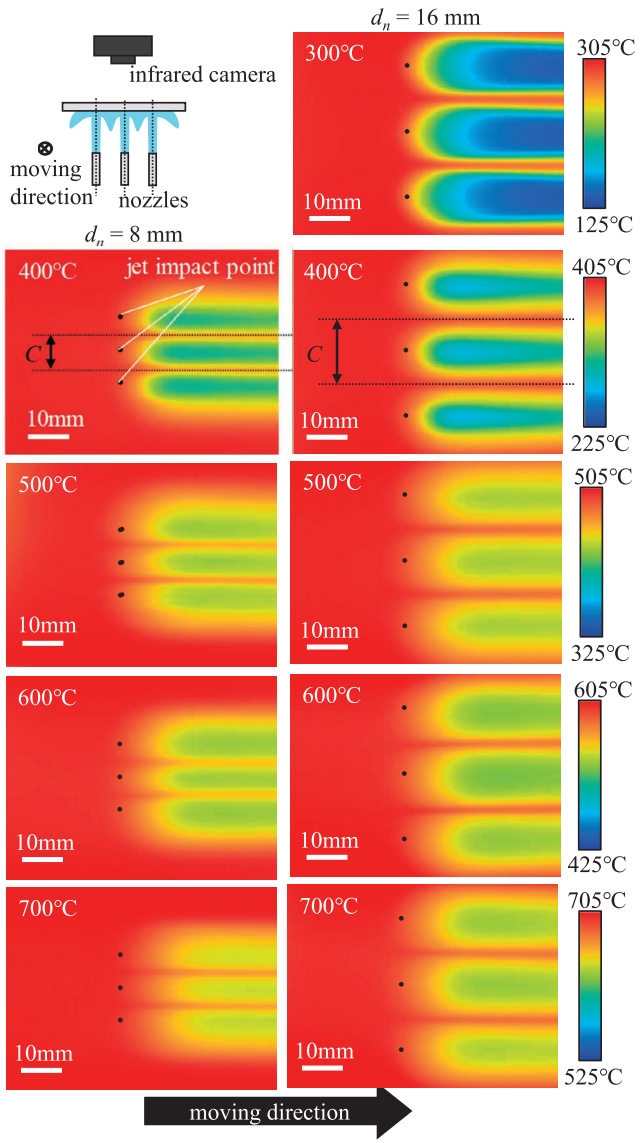

Fig. 4. Measured temperature profile on reverse surface.

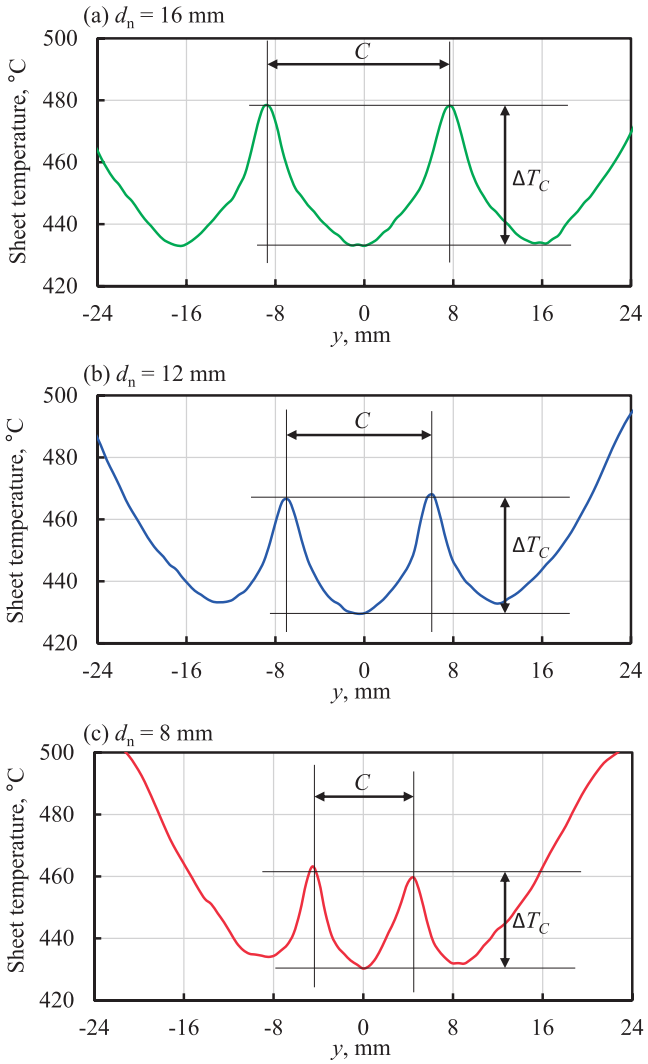

Fig. 5. Measured temperature distribution 30 mm away from jet impact point in the width direction at T_s = 500°C.

figure represent the estimated jet impact points. The temperature range of the color key between the minimum and maximum values is fixed at 175°C in all cases to enable a direct comparison of the temperature drop among the results. In the figures, three linear low-temperature areas stretch along the direction of motion from slightly downstream of the respective points of jet impact. The occurrence of the temperature drops downstream from (rather than at) the jet impact points can be attributed to the significant drop in the temperature of the sheet surface in the jet impact region of the cooled surface. As a result of heat conduction, this effect also occurred on the opposite side following some delay in time. As the test sheet moved some distance during this delay time, the temperature drop appeared downstream on the non-cooled surface rather than at the points of jet impact. In addition, relatively high-temperature areas were observed between adjacent pairs of low-temperature regions.

At T_s = 300°C, the temperature drop owing to jet impingement was very large because of the strong nucleate boiling. As the initial temperature of the test sheet was increased over the range T_s = 300–500°C, this temperature drop decreased, although at T_s = 600 and 700°C the temperature drop was slightly larger than at T_s = 500°C.

At d_n = 8 mm, the linear low-temperature area corresponding to the center jet appeared to narrow relative to the low-temperature areas corresponding to the two side jets because the liquid flow formed by the center jet impingement was confined between those formed by the two side jets. It was found that the width C of the cooling zone formed by the center jet impingement, as shown in the figure, was approximately equal to the nozzle spacing. Similar results were obtained at d_n = 12 and 16 mm, although the results for d_n = 12 mm are not shown.

The effect of varying the nozzle interval was investigated by comparing the measured temperature profiles in the width direction. **Figure 5** shows the measured temperature distributions 30 mm downstream from the jet impact point for T_s = 500°C; note that y = 0 mm denotes a line passing through the impact point of the center jet in the direction of motion (see also Fig. 3). As expected, three valleys and two peaks are observed in each result. The valley regions are formed by jet impingement. As explained above, the distance C between the two peaks is approximately equal to the nozzle interval. The temperature difference ΔT_C between the peaks and valleys is reduced at smaller values of C. Similar trends are observed at other test sheet temperatures.

Figure 6 shows the estimated heat flux distributions on the cooling surface obtained from inverse heat conduction analysis for experimental conditions coinciding with those shown in Figs. 2 and 4. There are three high heat flux regions around the jet impact points, indicating that a high degree of heat removal is achieved only in the jet impact regions whereas the other water film-covered regions are less cooled. The shapes of the three high heat flux regions are similar at d_n = 16 mm; at d_n = 8 mm, the high heat flux regions around the center jet are narrower in the width direction than those surrounding the two side-jets, indicating that the nozzle interval influences the heat transfer characteristics.

To investigate the effect of varying the nozzle interval on the heat transfer characteristics quantitatively, we calculated the total heat removal, Q_C, defined as the integral of local heat flux q over the center jet region as follows:

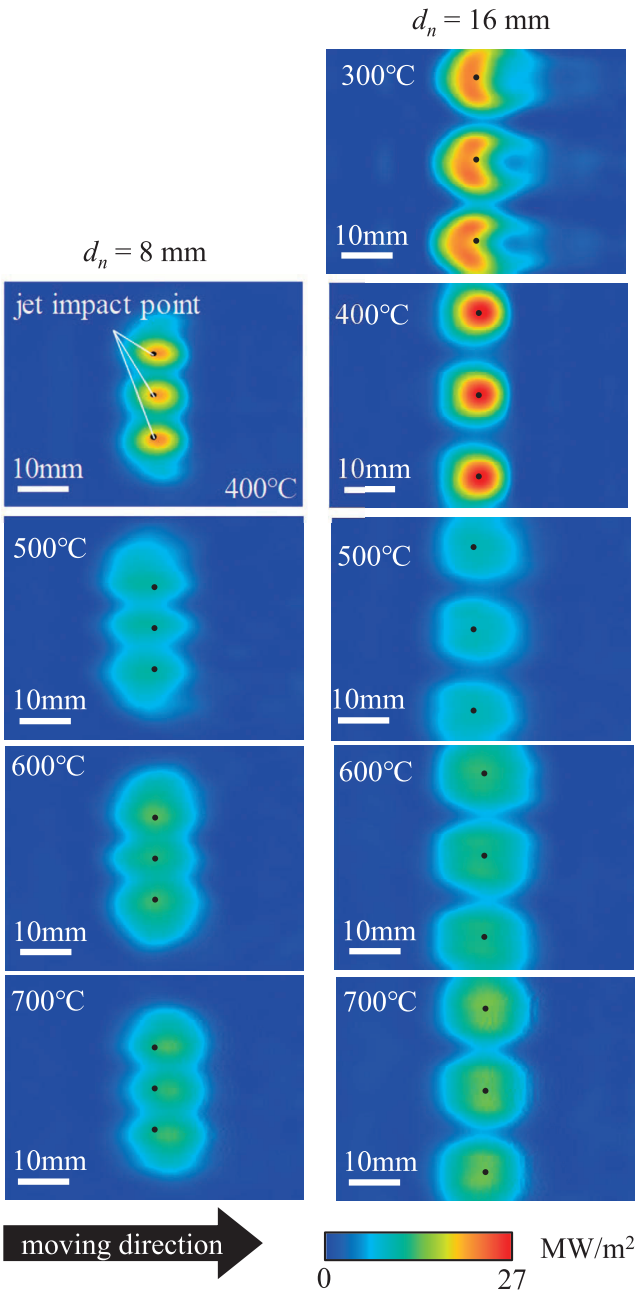

Fig. 6. Heat flux distributions.

$$Q_C = \int_S q\,dS, \quad \text{..... (3)}$$

where S is the area in which the total heat flux is equal to or larger than the threshold value, $q_{threshold}$, over the range C. Note that, although $q_{threshold}$ plays a role in capturing the "high heat flux region," there is no theoretical approach to determining an appropriate value of $q_{threshold}$. Furthermore, the total heat removal Q_C and area S vary depending on the choice of $q_{threshold}$. Namely, Q_C and S become large for small $q_{threshold}$, and vice versa. In this study, we evaluated Q_C using three values: $q_{threshold} = 1\times10^5$, 5×10^5, and 1×10^6 W/m^2. Fortunately, similar trends were observed at all threshold values. The following discussion of heat transfer characteristics is based on the Q_C obtained at $q_{threshold} = 1\times10^5$ W/m^2.

Figure 7 shows the total heat removal Q_C in the center jet region. It should be noted that the experiments were conducted for 10–20 runs at each experimental condition because some scattering of the measured temperature profiles was experimentally inevitable. The plotted symbols and error bars represent arithmetic mean values and standard deviations, respectively. The data corresponding to 300 and 350°C at d_n = 8 mm are missing because unwanted distortion of the steel sheets occurred. It is seen that Q_C varies depending on the temperature of the test sheet, reaching a minimum at 450°C for all nozzle intervals. In addition, Q_C is smaller at smaller nozzle intervals because reducing the interval reduces the area of integration of heat flux in Eq. (3); for the same reason, the range of error bars is larger at larger nozzle intervals.

These results suggest that the cooling ability at a given water flow rate deteriorates when a small nozzle interval is used. On the other hand, as shown in Fig. 5, a small nozzle interval can help achieve moderate uniform cooling along the width direction of the moving solid. These trends are consistent with the results obtained in our previous work for a downward-oriented set of three jets.[14] Thus, the choice of an appropriate nozzle interval is an important issue in designing actual cooling facilities in which upward and downward jet impingements are used.

To better understand these results, we introduce an index called "maximum heat flux," which is defined as the highest heat flux value in the domain of analysis. **Figure 8** shows

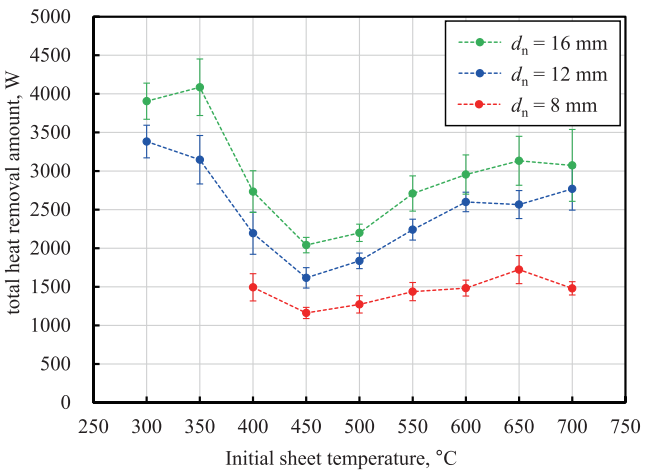

Fig. 7. Total amount of heat removal in the center jet region under upward triple-jet impingement.

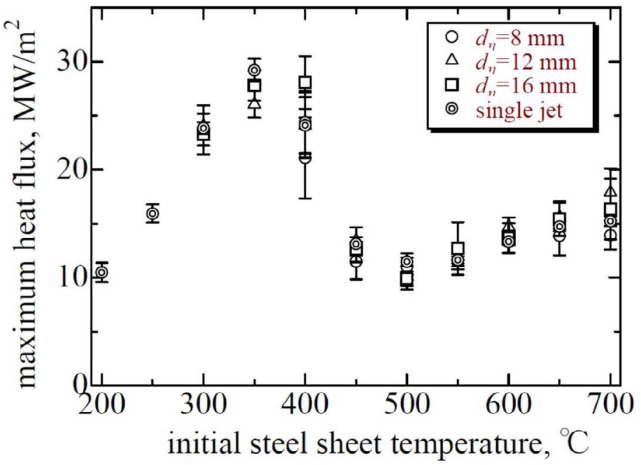

Fig. 8. Maximum heat flux. (Online version in color.)

the relationship between the initial temperature of the test sheet and the maximum heat flux in the center-jet region for the three-nozzle-interval cases assessed in this study. For reference, data for a single upward jet[15] are also plotted in the figure. Note that the experimental conditions under which the single-jet impingement data were obtained were nearly the same as those in this study except that only one jet was used and the nozzle-to-test sheet spacing was H = 10 mm. The plotted data show arithmetic mean values for 10–20 runs under the same experimental conditions, with the scatter bands indicating the standard deviations. It is also assumed that the heat transfer characteristics for single-jet impingement coincide with those in the center-jet region under a three-jet impingement with a sufficiently large nozzle interval.

At 400°C, there were significant differences among the four results as well as wide scatter bands for each value. Nevertheless, the experimental data over the entire temperature range follow an S-shaped trend that increases with the temperature of the test sheet before peaking at 350°C, decreases to a minimum at 500°C, and then increases again.

It should be noted that the position of maximum heat flux is fairly close to the jet impact point, indicating that the maximum heat flux corresponds to the dominant boiling mode in the jet impact region. In general, strong nucleate boiling is dominant in the jet impact region at $Ts \leq 350$°C and film boiling occurs at $Ts \geq 500$°C. In the middle region between these temperatures, the boiling mode can be categorized as transition boiling and there is a high degree of data scatter. These trends are consistent with the photographic observations of flow boiling shown in Fig. 2.

In the impact region around the center jet, the water flow are significantly affected by the momentum of the incoming jet and less influenced by the two side jets; this explains why the maximum heat flux is modestly independent of the number of jets and the nozzle interval. The results also suggest that heat transfer data obtained for single-jet impingement are applicable to multiple-jet impingement in the jet impact region but diverge from multiple-jet results outside of the jet impact region.

4. Conclusions

The cooling characteristics of a triple, upward-pointing water jet system impinging on a moving hot steel sheet were experimentally studied by varying the initial temperature of a test sheet and the jet interval. The findings are summarized as follows:

(1) Three elongated low-temperature regions were observed emanating from the jet impact points on the test sheet. The temperature drop in the low-temperature regions was found to be dependent on the initial temperature of the test sheet and associated with the boiling mode of water. In addition, at smaller jet intervals the low-temperature region formed by the center jet impingement was narrower, and the temperature variation was smaller, along the width direction.

(2) The heat flux was high only in the jet-impact regions. At small jet intervals, the high-heat-flux regions around the center jet were narrow in the width direction. In addition, the total heat removal calculated via integration of the local heat flux was smaller at smaller nozzle intervals.

(3) As the initial temperature of the test sheet increased, the maximum heat flux increased, reached a maximum, decreased to a minimum, and finally increased again. The results obtained for the triple- and single-jet systems followed similar trends under similar jet impact conditions.

REFERENCES

1) G. G. Guemo, V. Prodanovic and M. Militzer: *Steel Res. Int.*, **90** (2019), No. 4, 1800361. https://doi.org/10.1002/srin.201800361
2) P. Mishra, S. Nayak, P. Pradhan and D. Ghosh: *Interfacial Phenom. Heat Transf.*, **3** (2015), No. 2, 117. https://doi.org/10.1615/InterfacPhenomHeatTransfer.2014010574
3) C. Agrawal: *Steel Res. Int.*, **90** (2019), No. 1, 1800285. https://doi.org/10.1002/srin.201800285
4) L. Qiu, S. Dubey, F. H. Choo and F. Duan: *Int. J. Heat Mass Transf.*, **89** (2015), 42. https://doi.org/10.1016/j.ijheatmasstransfer.2015.05.025
5) V. S. Devahdhanush and I. Mudawar: *Int. J. Heat Mass Transf.*, **169** (2021), 120893. https://doi.org/10.1016/j.ijheatmasstransfer.2020.120893
6) C. F. Gomez, C. W. M. van der Geld, J. G. M. Kuerten, M. Bsibsi and B. P. M. van Esch: *Int. J. Heat Mass Transf.*, **163** (2020), 120545. https://doi.org/10.1016/j.ijheatmasstransfer.2020.120545
7) A. Mozumder, Y. Mitsutake and M. Monde: *Int. J. Heat Mass Transf.*, **68** (2014), 466. https://doi.org/10.1016/j.ijheatmasstransfer.2013.09.059
8) N. Nakata, T. Kuroki, A. Fujibayashi, Y. Hino and Y. Utaka: *ISIJ Int.*, **56** (2016), 294. https://doi.org/10.2355/isijinternational.ISIJINT-2015-454
9) M. Gradeck, A. Kouachi, J. Borean, P. Gardin and M. Lebouché: *Int. J. Heat Mass Transf.*, **54** (2011), No. 25–26, 5527. https://doi.org/10.1016/j.ijheatmasstransfer.2011.07.038
10) A. K. Sharma and S. K. Sahu: *Appl. Therm. Eng.*, **159** (2019), 113950. https://doi.org/10.1016/j.applthermaleng.2019.113950
11) M. Jahedi and B. Moshfegh: *Int. J. Heat Mass Transf.*, **137** (2019), 124. https://doi.org/10.1016/j.ijheatmasstransfer.2019.03.066
12) H. Fujimoto, K. Tatebe, Y. Shiramasa, T. Hama and H. Takuda: *ISIJ Int.*, **54** (2014), No. 6, 1338. https://doi.org/10.2355/isijinternational.54.1338
13) H. Fujimoto, Y. Shiramasa, K. Morisawa, T. Hama and H. Takuda: *ISIJ Int.*, **55** (2015), No. 9, 1994. https://doi.org/10.2355/isijinternational.ISIJINT-2015-124
14) H. Fujimoto, N. Hayashi, J. Nakahara, K. Morisawa, T. Hama and H. Takuda: *ISIJ Int.*, **56** (2016), No. 11, 2016. https://doi.org/10.2355/isijinternational.ISIJINT-2016-295
15) K. Morisawa, J. Nakahara, K. Nagata, H. Fujimoto, T. Hama and H. Takuda: *ISIJ Int.*, **58** (2018), No. 1, 140. https://doi.org/10.2355/isijinternational.ISIJINT-2017-383